On the global dynamics of Kirchhoff's equations : Rigid body models for underwater vehicles

Heinz Hanßmann and Philip Holmes

Program for Applied and Computational Mathematics
Princeton University, Princeton, NJ 08544–1000, U.S.A.

17 January 2001

Abstract

We study the Kirchhoff model for the motion of a rigid body submerged in an incompressible, irrotational, inviscid fluid in the absence of gravitational forces and torques. Symmetries allow reduction to a two degree–of–freedom Hamiltonian system. In [7] the existence and stability of pure and mixed mode equilibria was studied and, in [7] § 5.2, the system was averaged, allowing further reduction to one degree of freedom. We give an interpretation of the averaged Hamiltonian function as a normal form of order one. Iterating the process we obtain the normal form of order two, thus resolving a degeneracy noted in [7], and allowing us to prove that the (integrable) normal form of order two has heteroclinic orbits between 'pure 2' and between the 'pure 3' modes in a range of parameter values, and, at a critical (bifurcation) value, heteroclinic cycles linking pure 2 and pure 3 modes. We discuss the implications for the original system and the full rigid body motions.

1 Introduction

We study the dynamics of an ellipsoidal rigid body immersed in an ideal fluid, modelled by Kirchhoff's equations [8]. Our motivation stems from modelling the behaviour of an underwater vehicle when viscous effects are negligable. The simplest possible motions are pure modes, in which the body rotates about one of its principal axes, while translating along that axis. Stable pure modes represent desirable motions that require minimal control, and rapid maneuvers may be performed by destabilising such states and allowing the system to follow its uncontrolled dynamics. In this context, heteroclinic orbits connecting pure modes may help in the design of energy–efficient control strategies for vehicle reorientation.

For background on the Kirchhoff equations and the Hamiltonian setting, see [8, 9, 7]. The configuration space is the manifold $SE(3) = SO(3) \times \mathbb{R}^3$ of possible positions of *e.g.* the centre of mass in 3–space and of possible rotations of the body about the centre of mass. Correspondingly, the phase space is the cotangent bundle $T^*SE(3)$ equipped with the canonical 2–form. Following [7], we focus on the case of a neutrally buoyant body, in which the centre of mass coincides with the centre of volume and gravity exerts no net forces or torques. Then the Hamiltonian function is given solely by the kinetic energy and the system admits the full symmetry group $SE(3)$, acting by left translations. Dividing out this symmetry allows reduction to the quotient space

$$T^*SE(3)\big/_{SE(3)} \;\cong\; \mathfrak{se}(3)^* \;\cong\; \mathbb{R}^3 \times \mathbb{R}^3 \quad ,$$

where the Poisson structure is derived from the Lie bracket on $\mathfrak{se}(3)$. Denoting the co–ordinates of $\mathfrak{se}(3)^*$ by $(\pi_1, \pi_2, \pi_3, p_1, p_2, p_3)$, the Poisson bracket relations read

$$\begin{aligned} \{\pi_i, \pi_j\} &= -\epsilon_{ijk}\pi_k \\ \{\pi_i, p_i\} &= 0 \\ \{\pi_i, p_j\} &= -\epsilon_{ijk}p_k \\ \{p_i, p_j\} &= 0 \quad , \end{aligned} \tag{1}$$

where the alternating Levi–Civita symbol ϵ_{ijk} denotes the sign of the permutation $\binom{1\,2\,3}{i\,j\,k}$. The rank of this Poisson bracket (and thus the number of degrees of freedom) is two. Indeed, there are two *Casimirs* — functions that Poisson commute with all other functions — given by

$$\kappa_1(\pi, p) = (p \mid p) \qquad \text{and} \qquad \kappa_2(\pi, p) = (\pi \mid p) \quad ,$$

where $(\cdot \mid \cdot)$ denotes the inner product on $\mathbb{R}^3$. For subsequent use, we also define

$$\kappa_3(\pi, p) = \sqrt{(\pi \mid \pi)} \quad .$$

Given a Hamiltonian $H = H(\pi, p)$, Kirchhoff's equations read :

$$\dot{\pi} = \pi \times \nabla_\pi H \;+\; p \times \nabla_p H \tag{2}$$

$$\dot{p} = p \times \nabla_\pi H \quad . \tag{3}$$

We remark that p and π are the linear and angular momenta (or impulses) measured in a body frame of axes and refer to [9] for further details on the reduction process.

The kinetic energy is given by the inner product

$$H(\pi, p) \;=\; \frac{1}{2}\left(\binom{\pi}{p} \mid \mathbb{M}\binom{\pi}{p}\right) \quad , \tag{4}$$

where the symmetric 6×6 matrix $\mathbb{M}$ contains the *added inertia tensor*, the *added mass tensor* and coupling terms between linear and angular momenta. For ellipsoidal bodies, if the body frame coincides with the principal axes, $\mathbb{M}$ diagonalises to

$$\mathbb{M} \;=\; \begin{pmatrix} I_1 & 0 & 0 & 0 & 0 & 0 \\ 0 & I_2 & 0 & 0 & 0 & 0 \\ 0 & 0 & I_3 & 0 & 0 & 0 \\ 0 & 0 & 0 & m_1 & 0 & 0 \\ 0 & 0 & 0 & 0 & m_2 & 0 \\ 0 & 0 & 0 & 0 & 0 & m_3 \end{pmatrix}$$

and the Hamiltonian (4) becomes

$$H(\pi, p) \;=\; \frac{1}{2}\sum_{i=1}^{3}\frac{\pi_i^2}{I_i} \;+\; \frac{1}{2}\sum_{i=1}^{3}\frac{p_i^2}{m_i} \quad . \tag{5}$$

The mass and inertia terms derive from the lengths l_i of the three principal semi–axes of the ellipsoidal body, *cf.* [7, 9]. Throughout this paper, without loss of generality, we take $l_1 > l_2 \geq l_3$. Then $m_3 \geq m_2 > m_1$ and $I_2 > I_1$, but I_3 may be larger than, equal to, or smaller than both I_1 and I_2 .
The system admits the three reversing symmetries

$$\begin{aligned}
(\pi_1, \pi_2, \pi_3, p_1, p_2, p_3) &\mapsto (-\pi_1, \pi_2, \pi_3, -p_1, p_2, p_3) \\
(\pi_1, \pi_2, \pi_3, p_1, p_2, p_3) &\mapsto (\pi_1, -\pi_2, \pi_3, p_1, -p_2, p_3) \\
(\pi_1, \pi_2, \pi_3, p_1, p_2, p_3) &\mapsto (\pi_1, \pi_2, -\pi_3, p_1, p_2, -p_3) \quad .
\end{aligned} \tag{6}$$

Since combinations of these yield the (non–reversing) symmetries

$$\begin{aligned}
(\pi_1, \pi_2, \pi_3, p_1, p_2, p_3) &\mapsto (\pi_1, -\pi_2, -\pi_3, p_1, -p_2, -p_3) \\
(\pi_1, \pi_2, \pi_3, p_1, p_2, p_3) &\mapsto (-\pi_1, \pi_2, -\pi_3, -p_1, p_2, -p_3) \\
(\pi_1, \pi_2, \pi_3, p_1, p_2, p_3) &\mapsto (-\pi_1, -\pi_2, \pi_3, -p_1, -p_2, p_3) \quad ,
\end{aligned} \tag{7}$$

we conclude that, for fixed values $\kappa_1 = a^2$, $\kappa_2 = ab$ of the Casimirs, there are six (relative) equilibria $\pm(b, 0, 0, a, 0, 0)$, $\pm(0, b, 0, 0, a, 0)$ and $\pm(0, 0, b, 0, 0, a)$ of the (reduced) system. These are the *pure modes*, where the linear momentum is parallel to the angular momentum. As shown in [7] there exist further *mixed mode* equilibria in the cases $I_2 > I_3 \geq I_1$ and $I_2 > I_1 > I_3$. Figure 1 summarizes these findings in a bifurcation diagram with parameter $\gamma = |\frac{(\pi|p)}{(p|p)}| = |\frac{b}{a}|$, and shows stability types of the equilibria determined in [7].

As the parameter γ is varied, several bifurcations take place. At $\gamma = \gamma_{1\mathrm{H}}$ the pure 1 modes undergo a Hamiltonian Hopf bifurcation, where the value $\gamma_{1\mathrm{H}} > 0$ is given by

$$\gamma_{1\mathrm{H}}^2 \;=\; \frac{I_2 I_3}{I_2 + I_3 - I_1}\left[\mathcal{F}_1 + \sqrt{\mathcal{F}_1^2 - \mathcal{F}_2^2}\right]$$

with

$$\begin{aligned}
\mathcal{F}_1 &= \frac{2I_3 - I_1}{I_3}\left(\frac{1}{m_1} - \frac{1}{m_2}\right) + \frac{2I_2 - I_1}{I_2}\left(\frac{1}{m_1} - \frac{1}{m_3}\right) \\
\mathcal{F}_2 &= \frac{I_1}{I_3}\left(\frac{1}{m_1} - \frac{1}{m_2}\right) - \frac{I_1}{I_2}\left(\frac{1}{m_1} - \frac{1}{m_3}\right) \quad .
\end{aligned}$$

In the case $I_3 \geq I_2 > I_1$ this is the only local bifurcation to occur.

For $I_2 > I_3 \geq I_1$ there are Hamiltonian pitchfork bifurcations at $\gamma = \gamma_{3\mathrm{P}} = \alpha_{23} I_3$ and $\gamma = \gamma_{2\mathrm{P}} = \alpha_{23} I_2$, with $\alpha_{23} > 0$ given by

$$\alpha_{23}^2 \;=\; \frac{1}{I_2 - I_3}\left(\frac{1}{m_2} - \frac{1}{m_3}\right) \quad .$$

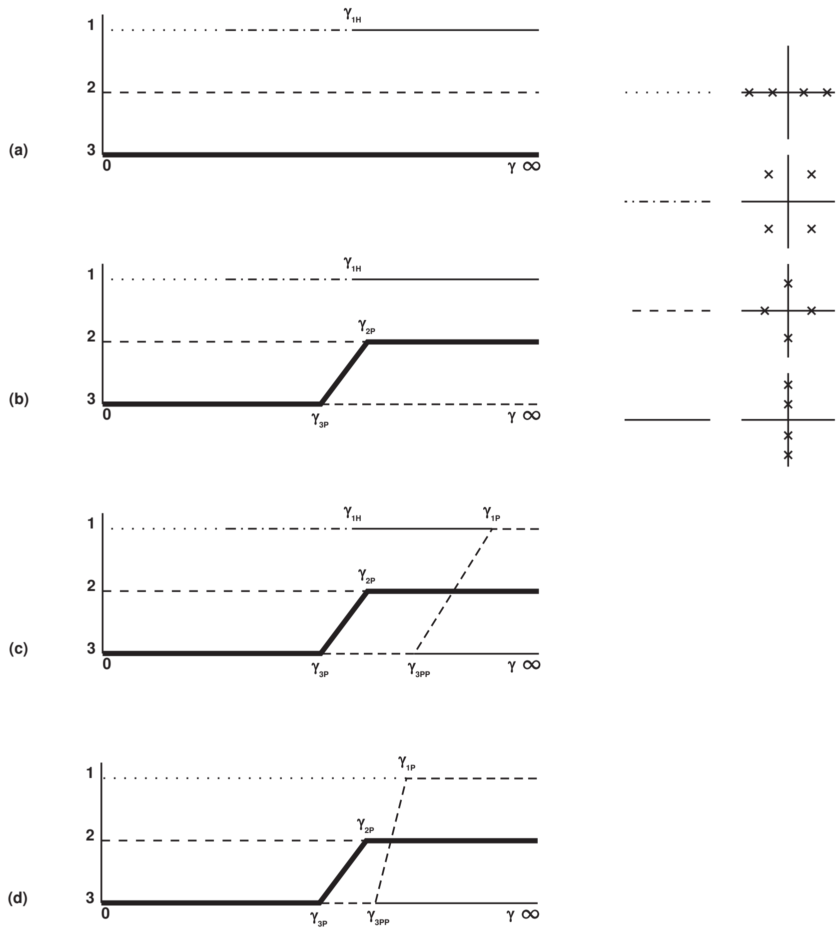

Figure 1: Pure and mixed mode equilibria. (a) $I_3 > I_2 > I_1$; (b) $I_2 > I_3 \geq I_1$; (c) $I_2 > I_1 > I_3$, small $I_1 - I_3$; (d) $I_2 > I_1 > I_3$, large $I_1 - I_3$. Solid lines indicate linearly stable (elliptic) equilibria ; dotted, chain–dotted and dashed lines indicate unstable equilibria with eigenvalues placements shown at right. Bold solid lines indicate nonlinearly stable equilibria determined by the Energy–Casimir method. Pitchfork bifurcation points are denoted $\gamma_{i\mathrm{P}}$, $\gamma_{i\mathrm{PP}}$ and Hopf bifurcation point $\gamma_{i\mathrm{H}}$. From [7].

At the first of these bifurcations the elliptic pure 3 modes become unstable, giving rise to four stable mixed 2-3 modes

$$(\pi, p) \quad = \quad (0, \pm\alpha_{23} I_2 p_2, \pm\alpha_{23} I_3 p_3, 0, p_2, p_3) \quad . \tag{8}$$

As γ increases from $\gamma_{3\mathrm{P}}$ to $\gamma_{2\mathrm{P}}$, the mixed 2-3 modes ‘approach’ the two pure 2 modes and reach them in the second Hamiltonian pitchfork bifurcation. Note that this scenario is governed by the symmetries (7).

At $\gamma = \gamma_{23\mathrm{C}} = \alpha_{23}\sqrt{I_2 I_3}$ the pure 2 and 3 modes are unstable *saddle–centers* and have the same energy, their energy–difference effectively changing sign as γ passes through this value. This suggests that there may be heteroclinic orbits between these pairs of modes, *i.e.* that a connection bifurcation takes place at $\gamma = \gamma_{23\mathrm{C}}$. The present paper was motivated by the desire to resolve this question.

If $I_2 > I_1 > I_3$, there are four additional branches of unstable mixed 1-3 modes

$$(\pi, p) \quad = \quad (\pm\alpha_{13} I_1 p_1, 0, \pm\alpha_{13} I_3 p_3, p_1, 0, p_3)$$

with $\alpha_{13} > 0$ given by

$$\alpha_{13}^2 \quad = \quad \frac{1}{I_1 - I_3}\left(\frac{1}{m_1} - \frac{1}{m_3}\right) \quad ,$$

extending between Hamiltonian pitchfork bifurcations at $\gamma = \gamma_{3\mathrm{PP}} = \alpha_{13} I_3$ and $\gamma = \gamma_{1\mathrm{P}} = \alpha_{13} I_1$. There are two (sub)cases according to whether $I_1 - I_3$ is small (and hence $\gamma_{1\mathrm{H}} < \gamma_{1\mathrm{P}}$) or large. In the latter case the pure 1 mode does not undergo a Hamiltonian Hopf bifurcation.

Homoclinic orbits are commonplace in Hamiltonian systems. Because of the reversing symmetries (6), heteroclinic orbits between symmetry–related hyperbolic equilibria are typical as well. In § 5.1 of [7] the existence of transverse homoclinic orbits to the pure 1 mode is shown in the nearly axisymmetric case $m_2 \approx m_3$, $I_2 \approx I_3$, implying that the system is non–integrable. In § 5.2 of [7] the Hamiltonian is formally averaged along the azimuthal angle of p with respect to π . The averaged system displays heteroclinic orbits connecting the pure $+2$ and -2 modes for $\gamma < \gamma_{23\mathrm{C}}$ and the pure $+3$ and -3 modes for $\gamma > \gamma_{23\mathrm{C}}$, but turns out to be degenerate for $\gamma = \gamma_{23\mathrm{C}}$. Thus it was not possible to conclude the existence of orbits connecting the four ± 2, ± 3 modes at this value. The present paper further considers this possibility, and, more generally, investiagates the global behavior of 'nearly spherical' vehicles for which $m_i \approx m_j$ and $I_i \approx I_j$.

This paper is organized as follows. In the next section we show that the averaged Hamiltonian obtained in [7] may be considered as a normal form of order one. We then compute the normal form of order two. Section 3 contains a partial analysis of these normal forms. In particular we show that the normal form of order two resolves the degeneracy of the normal form of order one. Furthermore, at $\gamma = \gamma_{23\mathrm{C}}$ there are heteroclinic cycles connecting the pure 2 and pure 3 modes for the normal form of order two. In Section 4 we discuss the consequences of these heteroclinic orbits. We summarize in Section 5.

2 Normalization of the Hamiltonian

The purpose of normalization is to perform a co–ordinate transformation that puts the 'lower order terms' in a simpler form. The small parameter ε measures how far the Hamiltonian H deviates from the well–understood Hamiltonian H_0^0 . In transformed co–ordinates, the normal form $\bar{H}$ of order n is then ε^{n+1}–close to H .

2.1 Theoretical background

Our aim is to find a co–ordinate transformation ψ that puts the system with Hamiltonian

$$H \;=\; H_0^0 \,+\, \varepsilon H_1^0$$

in normal form, up to order two. If ψ preserves the Poisson structure this means that the transformed system is generated by the Hamiltonian

$$H \circ \psi \;=\; H_0^0 \,+\, \varepsilon H_0^1 \,+\, \frac{\varepsilon^2}{2} H_0^2 \,+\, \mathcal{O}(\varepsilon^3) \quad ,$$

with $\{H_0^n, H_0^0\} = 0$ for $n = 1, 2$. A simple way to ensure that ψ is a Poisson map is to define it as the time–one–map of some Hamiltonian vector field with Hamiltonian W . Making the ansatz

$$W \;=\; \varepsilon W_1 \,+\, \frac{\varepsilon^2}{2} W_2 \quad ,$$

we obtain

$$\begin{aligned} H \circ \psi \;&=\; H \,+\, \{H, W\} \,+\, \frac{1}{2}\{\{H, W\}, W\} \,+\, \mathcal{O}(\varepsilon^3) \\ &=\; H_0^0 \,+\, \varepsilon H_1^0 \,+\, \varepsilon\{H_0^0, W_1\} \,+\, \frac{\varepsilon^2}{2}\{H_0^0, W_2\} \\ &\quad +\, \varepsilon^2\{H_1^0, W_1\} \,+\, \frac{\varepsilon^2}{2}\{\{H_0^0, W_1\}, W_1\} \,+\, \mathcal{O}(\varepsilon^3) \quad , \end{aligned}$$

whence

$$\{W_1, H_0^0\} \,+\, H_0^1 \;=\; H_1^0 \quad \text{and} \tag{9}$$

$$\{W_2, H_0^0\} \,+\, H_0^2 \;=\; 2\,\{H_1^0, W_1\}\} \,+\, \{\{H_0^0, W_1\}, W_1\} \quad . \tag{10}$$

We seek functions W_1, W_2 that solve these *homological equations*. To this end let $\mathcal{L}_{H_0^0} : F \mapsto \{F, H_0^0\}$ denote the Lie operator acting on elements $F \in \mathcal{F}$, where $\mathcal{F}$ is the space of (differentiable) Hamiltonian functions. Then H_0^1, H_0^2 are sought for in the kernel of $\mathcal{L}_{H_0^0}$. If $\mathcal{L}_{H_0^0}$ is semi–simple, the homological equations are easily solved since $\mathcal{F}$ splits into a direct sum

$$\operatorname{im} \mathcal{L}_{H_0^0} \oplus \ker \mathcal{L}_{H_0^0} \;=\; \mathcal{F} \quad .$$

Inverting the restriction of $\mathcal{L}_{H_0^0}$ to $\operatorname{im} \mathcal{L}_{H_0^0}$ then allows one to compute W_1 and W_2 . In particular we see that H_0^1 coincides with the average of H_1^0 along the flow generated by H_0^0 . This iterative procedure can be generalized to yield normal forms of any order, see [5, 3, 10].

2.2 Ingredients of the algorithm

In § 5.2 of [7] the Hamiltonian (5) is averaged along the periodic flow generated by $\kappa_3 = \sqrt{(\pi \mid \pi)}$ — this is done in a canonical co–ordinate system defined on each symplectic leaf $\kappa_1 = a^2$, $\kappa_2 = ab$. Here we prefer to work with

$$H_0^0 \;=\; \frac{1}{2I}(\pi \mid \pi) \;+\; \frac{1}{2m}(p \mid p) \;=\; \frac{\kappa_3^2}{2I} \;+\; \frac{\kappa_1}{2m}$$

(note that κ_3 and H_0^0 generate equivalent flows), since H_0^0 is ε–close to H with

$$\varepsilon \;=\; \max_i \left\{ \left|\frac{1}{I_i} - \frac{1}{I}\right| , \left|\frac{1}{m_i} - \frac{1}{m}\right| \right\} \quad .$$

Choosing I and m as convex combinations of the I_i and m_i , respectively implies that all mutual differences $\frac{1}{I_i} - \frac{1}{I_j}$ and $\frac{1}{m_i} - \frac{1}{m_j}$ are of order ε .

The key ingredient in computing the inverse of the Lie operator $\mathcal{L}_{H_0^0}$ on its image is to find diagonalising co–ordinates. Inspired by the variables given by (14)–(15) of [7], we define the complex co–ordinates

$$\begin{aligned}
\tau_1 &= \pi_1(\pi \mid p) - (\pi \mid \pi)p_1 \;+\; \mathrm{i}\sqrt{(\pi \mid \pi)}(\pi_2 p_3 - \pi_3 p_2) \\
\tau_2 &= \pi_2(\pi \mid p) - (\pi \mid \pi)p_2 \;+\; \mathrm{i}\sqrt{(\pi \mid \pi)}(\pi_3 p_1 - \pi_1 p_3) \\
\tau_3 &= \pi_3(\pi \mid p) - (\pi \mid \pi)p_3 \;+\; \mathrm{i}\sqrt{(\pi \mid \pi)}(\pi_1 p_2 - \pi_2 p_1)
\end{aligned}$$

and use $\kappa_1, \kappa_2, \kappa_3, \pi_1, \pi_2, \pi_3, \tau_1, \tau_2, \tau_3$ to embed our phase space in $\mathbb{R}^6 \times \mathbb{C}^3$. The Poisson structure on $\mathbb{R}^6 \times \mathbb{C}^3$ is chosen to make that embedding Poisson, *i.e.* κ_1, κ_2 are Casimirs and, in addition to (1), we have

$$\begin{aligned}
\{\kappa_3, \pi_i\} &= 0 && (11)\\
\{\kappa_3, \tau_i\} &= \mathrm{i}\tau_i && (12)\\
\{\pi_i, \tau_i\} &= 0 \\
\{\pi_i, \tau_j\} &= -\epsilon_{ijk}\tau_k && (13)\\
\{\tau_i, \tau_j\} &= 0 \\
\{\tau_i, \bar\tau_i\} &= 2\mathrm{i}\kappa_3(\kappa_1\pi_i^2 \;-\; 2\kappa_1\kappa_3^2 \;+\; \kappa_2^2) \\
\{\tau_i, \bar\tau_j\} &= 2\epsilon_{ijk}\left(\pi_k(2\kappa_1\kappa_3^2 - \kappa_2^2) \;+\; \mathrm{i}\,\kappa_1\kappa_3\pi_i\pi_j\right) \quad .
\end{aligned}$$

Specifically, in (14)–(15) of [7], the action–angle variables (r, s, ρ, σ) are defined, where $r = \sqrt{\pi_1^2 + \pi_2^2 + \pi_3^2} = \kappa_3$ and ρ is its conjugate angle, so that

$$\mathcal{L}_{H_0^0}(f) \;=\; \{f, H_0^0\} \;=\; \left\{f, \frac{r^2}{2I}\right\} \;=\; -\frac{r}{I}\frac{\partial f}{\partial \rho} \quad .$$

Thus, taking $f = r, s, e^{\mathrm{i}\rho}, e^{\mathrm{i}\sigma}$, we obtain

$$\mathcal{L}_{H_0^0}(f) \;=\; \lambda f \quad ,$$

with $\lambda = 0, 0, -\frac{\mathrm{i}r}{I}, 0$ respectively. The co–ordinate τ_1 effectively plays the rôle of $e^{\mathrm{i}\rho}$ and τ_2, τ_3 are included so that the Poisson bracket operation is closed (see (13)).

Counting dimensions, there are six independent relations between our co–ordinates at every point. An obvious candidate is

$$\kappa_3^2 \;=\; \pi_1^2 \;+\; \pi_2^2 \;+\; \pi_3^2 \quad ; \tag{14}$$

taking the Poisson bracket with the τ_i leads to further relations

$$\begin{aligned}
\pi_2\tau_3 - \pi_3\tau_2 &= \mathrm{i}\kappa_3\tau_1 \\
\pi_3\tau_1 - \pi_1\tau_3 &= \mathrm{i}\kappa_3\tau_2 \\
\pi_1\tau_2 - \pi_2\tau_1 &= \mathrm{i}\kappa_3\tau_3 \quad ,
\end{aligned}$$

and we encounter more relations in (16) below.
From (11)–(12) we have

$$\{\tau_i, H_0^0\} = -\frac{\mathrm{i}\kappa_3}{I}\tau_i \quad \text{and} \quad \{\pi_i, H_0^0\} = \{\kappa_i, H_0^0\} = 0 \quad ; \quad i = 1, 2, 3 \quad .$$

The Lie operator may therefore be written as

$$\mathcal{L}_{H_0^0} \;=\; \frac{-\mathrm{i}\,\kappa_3}{I}\left(\tau_1\frac{\partial}{\partial\tau_1} \;-\; \bar{\tau}_1\frac{\partial}{\partial\bar{\tau}_1} \;+\; \tau_2\frac{\partial}{\partial\tau_2} \;-\; \bar{\tau}_2\frac{\partial}{\partial\bar{\tau}_2} \;+\; \tau_3\frac{\partial}{\partial\tau_3} \;-\; \bar{\tau}_3\frac{\partial}{\partial\bar{\tau}_3}\right)$$

and thus maps a monomial

$$\mu \;=\; \kappa_1^{k_1}\kappa_2^{k_2}\kappa_3^{k_3}\pi_1^{k_4}\pi_2^{k_5}\pi_3^{k_6}\tau_1^{k_7}\tau_2^{k_8}\tau_3^{k_9}\bar{\tau}_1^{k_{10}}\bar{\tau}_2^{k_{11}}\bar{\tau}_3^{k_{12}}$$

to

$$\mathcal{L}_{H_0^0}(\mu) \;=\; \frac{-\mathrm{i}}{I}\left(k_7 + k_8 + k_9 - k_{10} - k_{11} - k_{12}\right)\kappa_3\mu \quad .$$

Here $k_3 \in \mathbb{Z}$ and all other $k_i \in \mathbb{N}_0$. For $\mu \in \mathrm{im}\,\mathcal{L}_{H_0^0}$ we obtain

$$\mathcal{L}_{H_0^0}^{-1}(\mu) \;=\; \frac{\mathrm{i}I\,\kappa_3^{-1}\mu}{k_7 + k_8 + k_9 - k_{10} - k_{11} - k_{12}} \quad .$$

Thus, while those terms in H_1^0 that are in the kernel of $\mathcal{L}_{H_0^0}$ form the normalized H_0^1 , the other monomials contribute to the generator W_1 , yielding

$$\begin{aligned}
W \;&=\; I\sum_{i=1}^{3}\left(\frac{1}{m_i} - \frac{1}{m}\right)\kappa_3^{-5}\mathrm{Im}\,\tau_i\left(\kappa_2\pi_i - \frac{1}{4}\mathrm{Re}\,\tau_i\right) \\
&=\; I\sum_{\substack{ijk \\ \text{cyclic}}}\left(\frac{1}{m_i} - \frac{1}{m}\right)\frac{\pi_j p_k - \pi_k p_j}{4(\pi \mid \pi)^2}\left(3(\pi \mid p)\pi_i + (\pi \mid \pi)p_i\right) \quad .
\end{aligned}$$

We remark that once W is known, the calculation of the transformed Hamiltonian $H \circ \psi = H_0^0 + \varepsilon H_0^1 + \mathcal{O}(\varepsilon^2)$ may equally be done in the (π, p) co–ordinates.

Functions in the kernel of $\mathcal{L}_{H_0^0}$ are invariant under the flow ϱ generated by H_0^0 . Kirchhoff's equations for H_0^0 are

$$\begin{aligned} \dot{\pi} &= 0 \\ \dot{p} &= p \times \pi \quad , \end{aligned} \tag{15}$$

revealing that the ring of ϱ–invariant functions is generated by $(p \mid p) = \kappa_1$, $(\pi \mid p) = \kappa_2$, π_1, π_2, π_3 . This yields the relations

$$\begin{aligned} \tau_i \bar{\tau}_i &= (\kappa_1 \kappa_3^2 - \kappa_2^2)(\kappa_3^2 - \pi_i^2) \\ \tau_i \bar{\tau}_j &= (\kappa_1 \kappa_3^2 - \kappa_2^2)(-\pi_i \pi_j + \mathrm{i}\epsilon_{ijk}\kappa_3 \pi_k) \quad . \end{aligned} \tag{16}$$

Note that $\kappa_1 \kappa_3^2 - \kappa_2^2 = (\pi \times p \mid \pi \times p)$. We now can compute the normal form of order one from the homological equation (9) as

$$H_0^0 + \varepsilon H_0^1 = \sum_{i=1}^{3} (\frac{1}{I_i} + \frac{(\pi \mid p)^2}{(\pi \mid \pi)^2} \frac{1}{m_i}) \frac{\pi_i^2}{2} + (\pi \times p \mid \pi \times p) \, F \quad , \tag{17}$$

with

$$F = \frac{1}{4(\pi \mid \pi)} (\frac{1}{m_1} + \frac{1}{m_2} + \frac{1}{m_3}) - \frac{1}{4(\pi \mid \pi)^2} \sum_{i=1}^{3} \frac{\pi_i^2}{m_i} \quad .$$

As shown in [2] the reversing symmetries (6) are preserved by the normalization procedure, whence the π_i only enter squared in (17).

To obtain the normal form of order two we must add to (17) the second order terms, computed from (10) :

$$\frac{\varepsilon^2}{2} H_0^2 = -I \frac{(p \mid p)(\pi \mid p)^2}{(\pi \mid \pi)^4} \sum_{i<j} \left(\frac{1}{m_i} - \frac{1}{m_j} \right)^2 \frac{\pi_i^2 \pi_j^2}{2} + (\pi \times p \mid \pi \times p) \, G \quad , \tag{18}$$

where G is a lengthy expression with two factors of the form $(\frac{1}{m_i} - \frac{1}{m})$ multiplying every term. We remark that there are terms of order three that also contain factors of the form $(\frac{1}{I_i} - \frac{1}{I})$. Computation of (17)–(18) was carried out in `Mathematica` [14]. Equation (17) coincides with the result of first order averaging in the (r, s, ρ, σ) co–ordinates of [7], § 5.2.

3 Dynamics of the normal forms

The normal form $\bar{H}$ depends on p only through the two Casimirs κ_1 and κ_2 . Explicitly writing $\bar{H} = \bar{H}(\kappa, \pi)$ leads to the equations of motion

$$\begin{aligned} \dot{\pi} &= \pi \times \nabla_\pi \bar{H} \\ \dot{p} &= p \times \nabla_\pi \bar{H} + \frac{1}{\kappa_3} \frac{\partial \bar{H}}{\partial \kappa_3} p \times \pi \quad . \end{aligned} \tag{19}$$

Using the relation (14) to make $\bar{H}$ a function of $\kappa_1, \kappa_2, \pi_1, \pi_2, \pi_3$ alone, the second set of equations again becomes simply

$$\dot{p} = p \times \nabla_\pi \bar{H} \quad , \tag{20}$$

the only difference from (3) being that H has been replaced by its normal form $\bar{H}$. As the right hand side of (20) is of the form $p \times \pi + \mathcal{O}(\varepsilon)$, these are 'fast' equations, while the 'slow' equations (19) decouple. This is of course the purpose of the normalization procedure : the function H_0^0 (and thus κ_3) becomes an integral of motion and we may reduce to single degree–of–freedom dynamics governed by (19), and subsequently solve for p by integrating (20).

The reduced phase space is $\mathbb{R}^3$ with Poisson structure (1). Correspondingly, κ_3 becomes a Casimir, and, having fixed the value $\kappa_3 = r$, solutions are confined to a 2–sphere of radius r . Before examining the normal form of order two, we review the results of [7] on the normal form of order one in the present context.

3.1 First order analysis

The Hamiltonian (17) coincides with that of a free rigid body with moments of inertia

$$J_i \;=\; \left(I_i^{-1} + \frac{a^2 b^2}{r^4} m_i^{-1} - \frac{a^2 r^2 - a^2 b^2}{2r^4} m_i^{-1} \right)^{-1} \tag{21}$$

after we subtract the combination of Casimirs

$$\frac{1}{4}(m_1^{-1} + m_2^{-1} + m_3^{-1})(\kappa_1 - \kappa_2^2 \kappa_3^{-2}) \quad .$$

Consequently, there are always six relative equilibria

$$(\pm r, 0, 0) \ , \ (0, \pm r, 0) \ , \ (0, 0, \pm r) \tag{22}$$

of (19). When $r = b$ these give rise to the pure modes of the full six averaged equations.

We are interested in heteroclinic orbits between these modes and therefore concentrate on $r = b$. Moreover, if $\pi \parallel p$ then the motion of p is also ε–slow since we are perturbing from (15). In fact, since p remains parallel to π , their dynamics are identical, implying that heteroclinic orbits of the reduced system (19) yield heteroclinic orbits of the full averaged system (19)–(20). Hence, connecting orbits exist between each pair of unstable pure modes as long as the three 'adjusted' moments of inertia J_1, J_2, J_3 all differ : we essentially have the classical free rigid body dynamics.

Note that, when $r = b$, the expression (21) simplifies to $J_i = (I_i^{-1} + (\gamma^2 m_i)^{-1})^{-1}$. Thus, for $I_2 > I_3 \geq I_1$ we have

$$J_2 = J_3 \quad \Leftrightarrow \quad \gamma = \gamma_{23\mathrm{C}} = \alpha_{23} \sqrt{I_2 I_3} \quad ,$$

and for $I_2 > I_1 > I_3$ we furthermore have

$$J_1 = J_3 \quad \Leftrightarrow \quad \gamma = \gamma_{13\mathrm{C}} = \alpha_{13} \sqrt{I_1 I_3} \quad .$$

In these cases an equator of the invariant sphere is filled with degenerate equilibria, and the scenarios (b) and (c) of figure 1 degenerate to (i) and (ii) of figure 2, respectively. Note that $\gamma_{3\mathrm{P}}$ (resp. $\gamma_{3\mathrm{PP}}$) and $\gamma_{2\mathrm{P}}$ (resp. $\gamma_{1\mathrm{P}}$) are ε–close to each other. Evidently the normal form of order one cannot adequately represent the behaviour on such small scales.

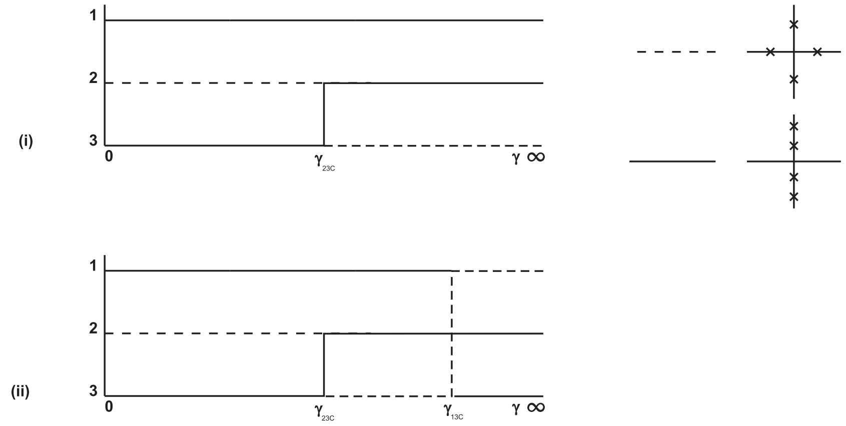

Figure 2: Degenerate bifurcation diagrams for equilibria of the first order normal form in the cases (i) $I_2 > I_3 \geq I_1$ and (ii) $I_2 > I_1 > I_3$. The Hamiltonian Hopf bifurcation of figure 1 does not appear in the normal form.

3.2 Second order analysis

Let $\bar{H}$ now denote the normal form of order two, *i.e.* the sum of (17) and (18). Again we focus on the dynamics on the $X_{\bar{H}}$–invariant submanifold $\{\pi \parallel p\}$ of $\mathbb{R}^3 \times \mathbb{R}^3$, first analysing the reduced system (19) on the 2–sphere S_b^2 of radius $r = b$ and then reconstructing the solution of (20) by setting $p(t) = \frac{a}{r}\pi(t) = \frac{\pi(t)}{\gamma}$.
For $\pi \parallel p$ the normal form of order two reduces to

$$\bar{H}_{a,b}(\pi) \;=\; \sum_{i=1}^{3}\left(\frac{1}{I_i} + \frac{1}{\gamma^2 m_i}\right)\frac{\pi_i^2}{2} \;-\; \frac{I}{\gamma^4 b^2}\sum_{i<j}\left(\frac{1}{m_i} - \frac{1}{m_j}\right)^2\frac{\pi_i^2\pi_j^2}{2}$$

and the (non–oriented) solution curves are given by the intersections $S_b^2 \cap \{\bar{H}_{a,b} = h\} \subseteq \mathbb{R}^3$. Most orbits are periodic, while those points where the two surfaces touch are equilibria. Furthermore, there are homoclinic and heteroclinic orbits to hyperbolic equilibria, *cf.* figure 3.
Seeking critical points of $\bar{H}_{a,b}$ on S_b^2 we are led to the equations

$$\begin{aligned}
\left[\frac{1}{I_1} + \frac{1}{\gamma^2 m_1} - \frac{I}{\gamma^4}\left(\left(\frac{1}{m_1} - \frac{1}{m_2}\right)^2\frac{\pi_2^2}{b^2} + \left(\frac{1}{m_1} - \frac{1}{m_3}\right)^2\frac{\pi_3^2}{b^2}\right)\right]\pi_1 &= \lambda\pi_1 \\
\left[\frac{1}{I_2} + \frac{1}{\gamma^2 m_2} - \frac{I}{\gamma^4}\left(\left(\frac{1}{m_2} - \frac{1}{m_1}\right)^2\frac{\pi_1^2}{b^2} + \left(\frac{1}{m_2} - \frac{1}{m_3}\right)^2\frac{\pi_3^2}{b^2}\right)\right]\pi_2 &= \lambda\pi_2 \\
\left[\frac{1}{I_3} + \frac{1}{\gamma^2 m_3} - \frac{I}{\gamma^4}\left(\left(\frac{1}{m_3} - \frac{1}{m_1}\right)^2\frac{\pi_1^2}{b^2} + \left(\frac{1}{m_3} - \frac{1}{m_2}\right)^2\frac{\pi_2^2}{b^2}\right)\right]\pi_3 &= \lambda\pi_3
\end{aligned}$$

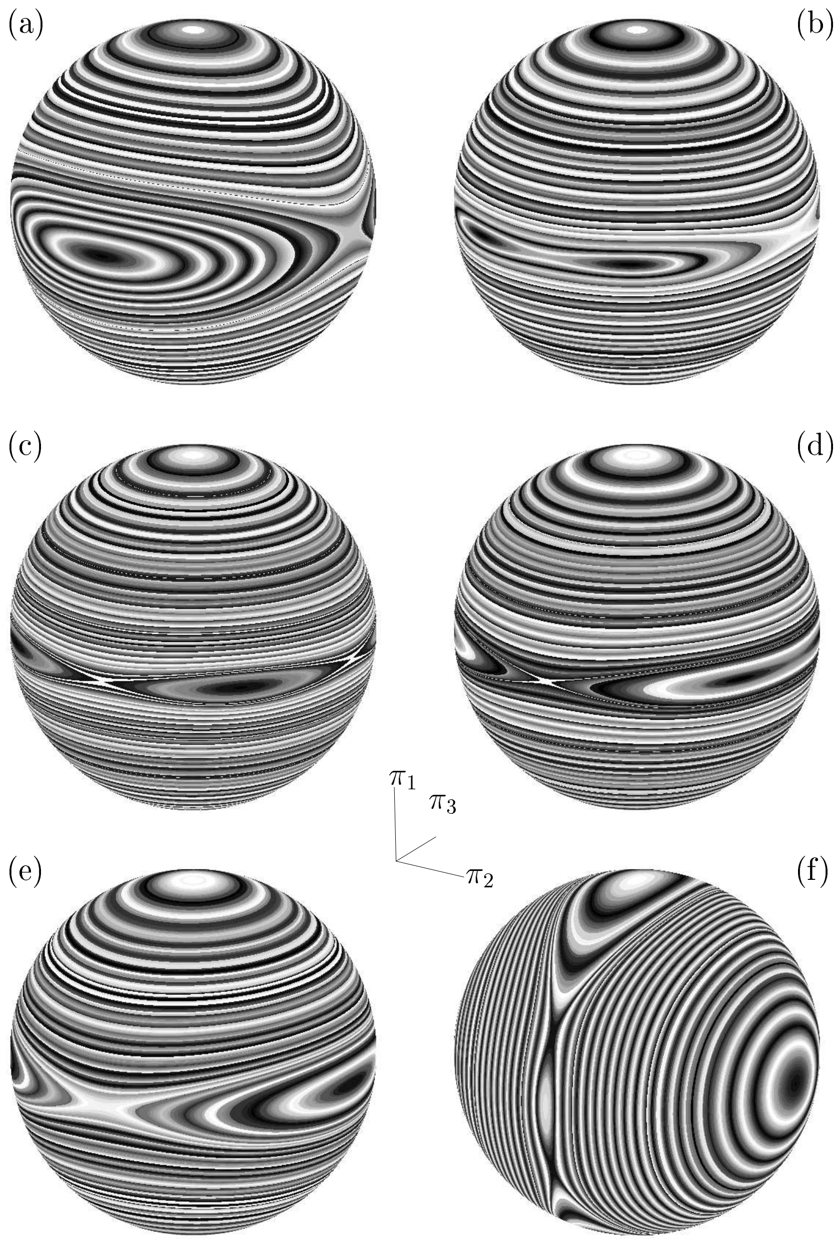

Figure 3: Phase portraits of the reduced order two system on S_b^2 : (a)–(e) the cases $I_2 > I_3 \geq I_1$ and $I_2 > I_1 > I_3$, with γ increasing from below γ_- to above γ_+ , mass and inertia values as specified in Section 4.2 ; (f) the case $I_2 > I_1 > I_3$ with $\gamma \in \,]\check{\gamma}_-, \check{\gamma}_+[$, same mass and inertia values except for $I_1 = 9.7$. See text for further details.

where λ is a Lagrange parameter. We immediately conclude that the points (22) are equilibria of the normal form of order two as well. Since $I_2 > I_1$ there are no valid solutions (π_1, π_2, π_3) with both π_1 and π_2 nonzero.

If $I_2 > I_3$ we may eliminate λ from the last two equations and obtain four additional equilibria $(0, \pm\hat{\pi}_2, \pm\hat{\pi}_3)$ for $\gamma = |\frac{b}{a}|$ in the open interval $]\gamma_-, \gamma_+[$ with

$$\gamma_\pm^2 \;=\; \alpha_{23}^2 I_2 I_3 \left(\frac{1}{2} + \frac{1}{2}\sqrt{1 \pm 4(\frac{I}{I_3} - \frac{I}{I_2})} \right) \quad . \tag{23}$$

At γ_- and γ_+ the equilibria $(0,0,\pm b)$ and $(0,\pm b,0)$ undergo Hamiltonian pitchfork bifurcations, respectively, see figure 3(a)–(b) and (d)–(e). Note that the values (23) are ε^2–close to $\gamma_{3\mathrm{P}}^2$ and $\gamma_{2\mathrm{P}}^2$, while the normalizing co–ordinate transformation ψ maps

$$(0, \pm\hat{\pi}_2, \pm\hat{\pi}_3, 0, \frac{\pm\hat{\pi}_2}{\gamma}, \frac{\pm\hat{\pi}_3}{\gamma}) \tag{24}$$

into an ε^2–neighbourhood of (8). Hence (24) correspond to the mixed 2-3 modes of the original system. At $\gamma = \gamma_{23\mathrm{C}}$ we have $\bar{H}_{a,b}(0,\pm b,0) = \bar{H}_{a,b}(0,0,\pm b)$ and all four of these (hyperbolic) equilibria — the pure 2 and pure 3 modes — are connected in a heteroclinic cycle, see figure 3(c).

The whole $X_{\bar{H}}$–invariant subspace $\{\pi \parallel p\}$ of $\mathbb{R}^3 \times \mathbb{R}^3$ consists of critical values $(\bar{H}, \kappa_1, \kappa_2, \kappa_3) = (h, a^2, ab, b)$ of the energy–momentum mapping $(\bar{H}, \kappa)$. To obtain an overview of these dynamics we therefore consider

$$(\bar{H}, \frac{\kappa_3}{\sqrt{\kappa_1}} = \gamma) \;:\; \mathbb{R}^3 \times \mathbb{R}^3 \backslash \{0\} \;\longrightarrow\; \mathbb{R}^2 \quad . \tag{25}$$

The set Σ of critical values (h, γ) of (25) is sketched in figure 4(i) (*cf.* figure 1(b)).
If $I_1 > I_3$ there are four further equilibria $(\pm\check{\pi}_1, 0, \pm\check{\pi}_3)$ for $\gamma \in]\check{\gamma}_-, \check{\gamma}_+[$ with

$$\check{\gamma}_\pm^2 \;=\; \alpha_{13}^2 I_1 I_3 \left(\frac{1}{2} + \frac{1}{2}\sqrt{1 \pm 4(\frac{I}{I_3} - \frac{I}{I_1})} \right) \quad ,$$

which correspond to the mixed 1-3 modes. However, the scenario is different here, since these equilibria are hyperbolic while the equilibria (22) are all elliptic. It is therefore now the *mixed* 1-3 modes that are connected in a heteroclinic cycle throughout $]\check{\gamma}_-, \check{\gamma}_+[$. In case $\gamma_+ < \check{\gamma}_-$ the symmetries (7) ensure that the flows for these γ are all equivalent to that depicted in figure 3(f). The critical values (h, γ) are shown in figure 4(ii) for this case ; note, however, that the (additional) intersection of the pure mode 1 and 3 branches does not correspond to a bifurcation. In case $\gamma_{23\mathrm{C}} > \check{\gamma}_-$ the two bifurcation sequences interact, resulting in fourteen coexisting equilibria (eight elliptic and six hyperbolic) and a heteroclinic cycle between the pure 2 and the mixed 1-3 modes.

We end by noting that the (r, s, ρ, σ) variables used in [7] are singular at $\pi_1 = \pm r$ — (s, σ) provide cylindrical co–ordinates on S_b^2 — and thus that the full phase portraits of figure 3 could not be deduced from normalized sytems in those co–ordinates.

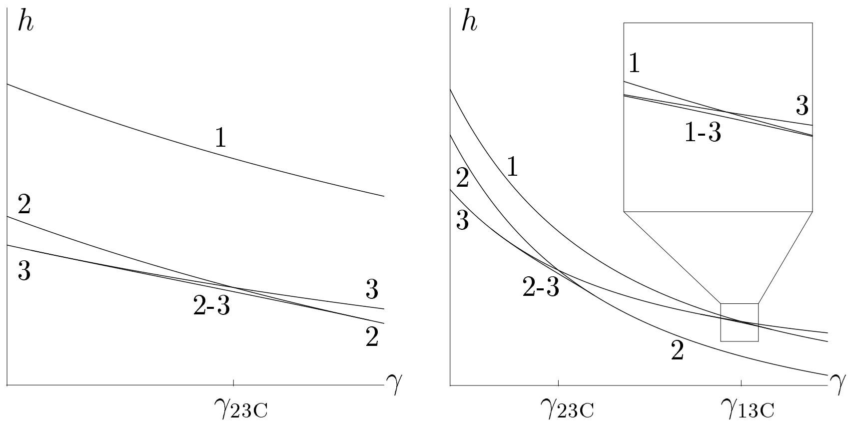

Figure 4: The set of critical values of (25) : a bifurcation diagram plotted in terms of energy : (i) $I_2 > I_3 > I_1$; (ii) $I_2 > I_1 > I_3$ and $\gamma_+ < \check{\gamma}_-$. Mass and inertia values as for figure 3(a)–(e) and (f) respectively.

4 Implications for the original system

After the co–ordinate transformation ψ , the Hamiltonian of (5) is ε^3–close to the normal form $\bar{H}$ of order two given by (17)–(18). Hence, by the usual averaging theorem (*e.g.* [6]), solutions of the original Kirchhoff equations follow those of the normalized sytem with Hamiltonian $\bar{H}$ within $\mathcal{O}(\varepsilon^2)$ for times of $\mathcal{O}(\frac{1}{\varepsilon})$. However, in this case the dimension reduction implicit in the normalization procedure allows us to draw stronger conclusions. We describe these first for the model equations and then for the physical application.

4.1 Dynamics of the Kirchhoff equations

Since the phenomena decribed in Section 3 are structurally stable in the space of single degree–of–freedom Hamiltonian systems, and further normalization at successively higher order preserves invariance of κ_3 , these behaviours persist in normal forms $\bar{H}$ of *arbitrarily* high order. We may therefore conclude that, up to 'splitting' terms smaller than ε^n for any n , *e.g.* heteroclinic cycles among the pure 2 and 3 and the mixed 1-3 modes exist for parameter values near those given. More generally, the full dynamics tracks those of the completely integrable system $\bar{H}$ with errors smaller than ε^n for any n . All these conclusions are, of course, predicated on the assumption that the (added) mass and inertia values are 'nearly equal' :

$$\varepsilon \quad = \quad \max_{i,j} \left\{ |\frac{1}{I_i} - \frac{1}{I_j}| \, , \, |\frac{1}{m_i} - \frac{1}{m_j}| \right\} \quad \ll \quad \frac{1}{I} \quad . \tag{26}$$

In contrast, in [7], it was only assumed that (26) held for $i, j = 2, 3$ and m_1 and I_1 were allowed to differ from m_2, m_3 and I_2, I_3 respectively by large amounts. This is why the averaging of [7] § 5.2 is only formal.

We remark that, in addition to the heteroclinic orbits to and cycles among the pure and mixed modes discussed above, the phase portraits of figure 3(b)–(d) also reveal homoclinic loops to the (unstable) pure 2 and pure 3 modes. These will also persist up to small splitting terms.

4.2 Results for underwater vehicles

Unfortunately, the more stringent condition (26) implies that we may only draw rigorous conclusions regarding nearly–spherical vehicles, rather than for the broader class of nearly–axisymmetric, elongated (cigar–shaped) vehicles considered in [7], which are more appropriate for modelling typical streamlined underwater bodies.

The heteroclinic cycle of figure 3(c) only occurs when $I_2 > I_3$. The constants $m_1, m_2, m_3, I_1, I_2, I_3$ of a given ellipsoidal underwater vehicle are not independent, but all derive from the lengths $l_1 > l_2 \geq l_3$ of the principal semi–axes. In [7] a perturbation analysis from the axisymmetric case yields a threshold $\frac{l_1}{l_2} > 1.62$ for passing from $I_3 > I_2 > I_1$ to $I_2 > I_3 > I_1$. On the other hand, the more the l_i differ, the larger the differences $m_i - m_j$ will be. It is therefore not *a priori* clear that an underwater vehicle displaying heteroclinic cycles indeed exists.

We therefore considered the example $l_1 = 0.5$, $l_2 = 0.3$, $l_3 = 0.2$ in more detail ; here $m_1 \approx 158.4$, $m_2 \approx 166.2$, $m_3 \approx 278.7$, $I_1 \approx 5.120$, $I_2 \approx 10.71$, $I_3 \approx 8.707$ and choosing $I = 6.928$ the relevant 'small' parameter (26) reads $\varepsilon I \approx 0.707$. Thus, the normal form of order two is still a poor approximation, but can be improved upon by working with a normal form of (very) high order. While the actual computation of such a normal form is not feasable, it suffices for us that this implies the existence of heteroclinic cycles in the full system up to splitting terms smaller than any algebraic order. Correspondingly, for the mass and inertia values given above, we were able to find the scenario of figure 3(a)–(e) numerically, see figure 5(a)–(d). These are computed with $\kappa_3 = \|\pi\| \approx 1$ and $\sqrt{\kappa_1} = \|p\|$ varying from 3 to 4 , corresponding to an $\mathcal{O}(\varepsilon^3)$ error of approximately 1.8×10^{-5} . This accounts for the close agreement between actual stable and unstable manifolds and those approximated by the normalized system. However, the physical velocities corresponding to these momenta are very low (50–100 m/h). Higher speeds would reveal more significant splitting of the manifolds.

The linear momentum is fixed in inertial space. A motion corresponding to the heteroclinic cycle therefore results in a rearrangement of the body–axis aligning with that direction. We refer to [7] § 6 for a detailed description of the full 12–dimensional underwater vehicle motion.

Kirchhoff's equations are an idealisation that neglects viscous effects and, more significantly, assumes full pressure recovery and no separated flow, *cf.* [8]. This is reasonable for slender (cigar–shaped) bodies, but not for nearly spherical bodies travelling at realistic speeds. Addition of (phenomenological) models for separation–induced drag would

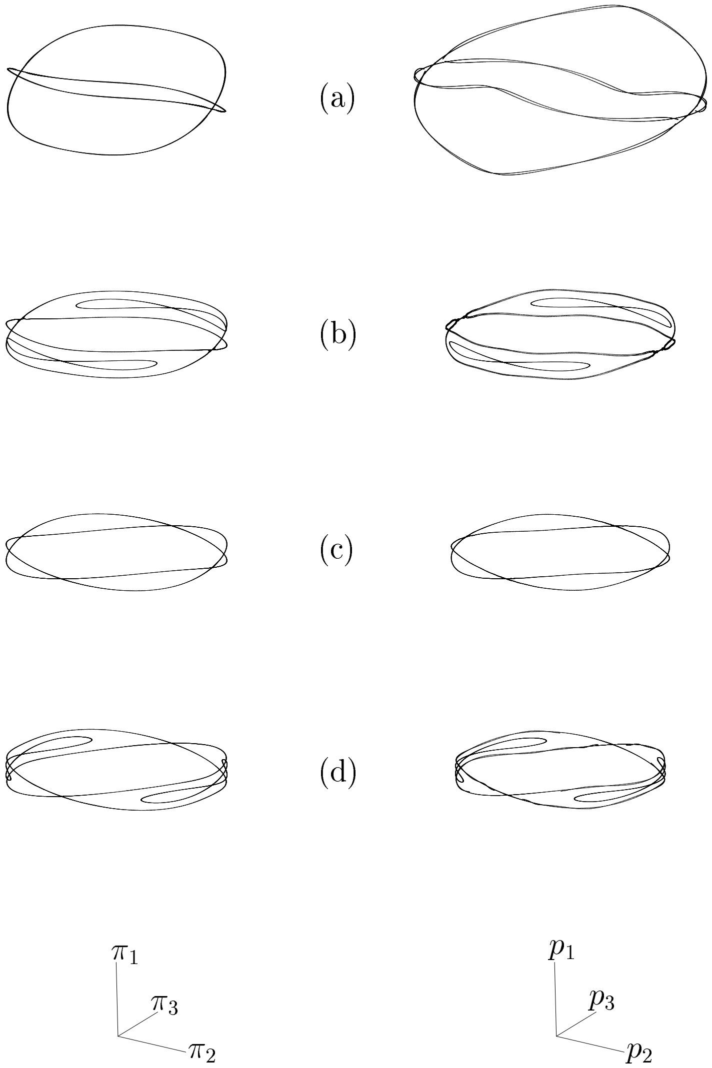

Figure 5: Projections of orbits of the full system for $l_1 = 0.5$, $l_2 = 0.3$, $l_3 = 0.2$ to the π–space (left) and p–space (right, scaled 1:3). Here we use initial conditions satisfying $\|\pi\| = b = 1$ and start solutions close to the pure 2 and 3 modes with $\kappa_1 = a^2$ and $\kappa_2 = ab$ chosen such that : (a) $\gamma = |\frac{b}{a}| = 0.25 < \gamma_{3\mathrm{P}}$, (b) $\gamma = 0.32 \in]\gamma_{3\mathrm{P}}, \gamma_{23\mathrm{C}}[$, (c) $\gamma = 0.336037 \approx \gamma_{23\mathrm{C}}$, (d) $\gamma = 0.35 \in]\gamma_{23\mathrm{C}}, \gamma_{2\mathrm{P}}[$. Compare with figure 3.

introduce non–Hamiltonian perturbations that cannot be included in the present analysis.

5 Conclusions

In this paper we have carried out normalization up to second order for the Kirchhoff equations (2)–(3) modelling the dynamics of a nearly–spherical body submerged in an incompressible, inviscid fluid of infinite extent. By effectively averaging along the fast, integrable flow of the spherical case, we find that solutions are approximated, up to terms of arbitrarily small algebraic order, by those of a completely integrable system (with lowest order terms (19)–(20)) whose angular and linear momentum components decouple. The resulting reduced dynamics may be pictured as flows on an (approximately) constant angular momentum sphere, restricted to intersections of that sphere with the normalized Hamiltonian. The phase portraits typically contain six, ten or fourteen equilibria and the hyperbolic equilibria have heteroclinic or homoclinic orbits (figure 3). This permits us to carry out a complete global analysis of the normalized system, and to conclude that the Kirchhoff equations have families of nearly heteroclinic cycles connecting certain pure and mixed mode relative equilibria, in appropriate parameter ranges. We suggest that such cycles provide 'channels' in the natural dynamics that will be useful in obtaining energy–efficient reorientation maneuvers of underwater vehicles.

In conclusion, we remark that the analysis of an averaged, effectively two–dimensional flow carried out here is similar in spirit to Floris Takens' own studies of unfoldings of co–dimension two bifurcations of Poincaré return maps in periodically forced oscillations [13], *cf.* [12]. In 1974 the chance discovery of these (still generally unpublished) lecture notes, in the library of the Institute of Sound and Vibration Research at Southampton University, enormously encouraged and helped the second author in his fumbling attempts to learn bifurcation theory and apply it to problems in engineering. Some fifteen years later, the first author found these same two lecture notes very helpful in his 'first steps' in dynamical systems. We therefore believe that the present paper is an especially suitable tribute to an inspiring teacher, colleague, and friend.

Acknowledgements

We thank Naomi Leonard for helpful discussions and for sharing her code for computation of added masses and moments of inertia, and John Schmitt, Britta Sommer, Wolf Jung, John Vincent and Jeff Moehlis for helping produce figures 2, 3 and 5. The figures were made using the programs `gnuplot` [4], `CorelDRAW`, `ESFERAS` [11], `Mathematica` [14] and `DsTool` [1]. HH thanks the Max Kade Foundation for a fellowship that supported his visit to Princeton. PH thanks the US Department of Energy for partial support under DoE: DE-FG02-95ER25238.

References

[1] Back A, Guckenheimer J, Myers M, Wicklin F and Worfolk P 1992 "*dstool :* Computer Assisted Exploration of Dynamical Systems" Notices Amer. Math. Soc. **39** p 303–309

[2] Churchill R C, Kummer M and Rod D L 1983 "On averaging, reduction, and symmetry in Hamiltonian systems" J. Diff. Eq. **49** p 359–414

[3] Deprit A 1969 "Canonical Transformations Depending on a Small Parameter" Cel. Mech. **1** p 12–30

[4] URL `http://www.gnuplot.org`

[5] Gröbner W 1967 *Die Lie–Reihen und ihre Anwendungen* (Berlin : Deutscher Verlag der Wissenschaften)

[6] Guckenheimer J and Holmes P 1983 *Nonlinear Oscillations, Dynamical Systems and Bifurcations of Vector Fields* (New York : Springer Verlag)

[7] Holmes P, Jenkins J and Leonard N E 1998 "Dynamics of the Kirchhoff equations I : Coincident centers of gravity and buoyancy" Physica D **118** p 311–342

[8] Lamb H 1932 *Hydrodynamics* (Cambridge : Cambridge University Press)

[9] Leonard N E 1997 "Stability of a bottom–heavy underwater vehicle" Automatica **33** p 1–11

[10] Meyer K R and Hall G R 1992 *Introduction to Hamiltonian dynamical systems and the N–body problem* (New York : Springer Verlag)

[11] Pascua P, Rubio J L, Viartola A and Ferrer S 1996 "Visualizing Relative Equilibria and Bifurcations by Painting Hamiltonians on Personal Computers" Int. J. Bifurcation Chaos Appl. Sci. Eng. **6** p 1411–1424

[12] Takens F 1973 *Introduction to Global Analysis* (Utrecht : Communications of the Mathematical Institute, Rijksuniversiteit Utrecht, 1973-2)

[13] Takens F 1974 *Applications of Global Analysis* (Utrecht : Communications of the Mathematical Institute, Rijksuniversiteit Utrecht, 1974-3)

[14] Wolfram S 1996 *The Mathematica Book* (Cambridge : Cambridge University Press)